



A study of the Fermi–Pasta–Ulam problem in dimension two

Giancarlo Benettin and Giacomo Gradenigo

Citation: *Chaos: An Interdisciplinary Journal of Nonlinear Science* **18**, 013112 (2008); doi: 10.1063/1.2838458

View online: <http://dx.doi.org/10.1063/1.2838458>

View Table of Contents: <http://scitation.aip.org/content/aip/journal/chaos/18/1?ver=pdfcov>

Published by the [AIP Publishing](#)



Re-register for Table of Content Alerts

Create a profile.



Sign up today!



A study of the Fermi–Pasta–Ulam problem in dimension two

Giancarlo Benettin^{1,a)} and Giacomo Gradenigo^{2,b)}

¹Dipartimento di Matematica Pura e Applicata, Università di Padova, Via G. Belzoni 7, 35131 Padova, Italy

²Dipartimento di Fisica, Università di Trento, Via Sommarive 14, 38100 Povo, Italy

(Received 26 September 2007; accepted 9 January 2008; published online 10 March 2008)

Continuing the previous work on the same subject, we study here different two-dimensional Fermi–Pasta–Ulam (FPU)-like models, namely, planar models with a triangular cell, molecular-type potential and different boundary conditions, and perform on them both traditional FPU-like numerical experiments, i.e., experiments in which energy is initially concentrated on a small subset of normal modes, and other experiments, in which we test the time scale for the decay of a large fluctuation when all modes are excited almost to the same extent. For each experiment, we observe the behavior of the different two-dimensional systems and also make an accurate comparison with the behavior of a one-dimensional model with an identical potential. We assume the thermodynamic point of view and try to understand the behavior of the system for large n (the number of degrees of freedom) at fixed specific energy $\varepsilon = E/n$. As a result, it turns out that: (i) The difference between dimension one and two, if n is large, is substantial. In particular (making reference to FPU-like initial conditions) the “one-dimensional scenario,” in which the dynamics is dominated for a long time scale by a weakly chaotic metastable situation, in dimension two is absent; moreover in dimension two, for large n , the time scale for energy sharing among normal modes is drastically shorter than in dimension one. (ii) The boundary conditions in dimension two play a relevant role. Indeed, models with fixed or open boundary conditions give fast equipartition, on a rather short time scale of order ε^{-1} , while a periodic model gives longer equilibrium times (although much shorter than in dimension one). © 2008 American Institute of Physics. [DOI: [10.1063/1.2838458](https://doi.org/10.1063/1.2838458)]

This paper concerns the Fermi–Pasta–Ulam (FPU) problem in dimension two, and should be considered as a continuation of Ref. 1 in this journal (familiarity with Ref. 1 however, is not assumed). The model studied in Ref. 1 is a two-dimensional lattice with a triangular cell, overall hexagonal shape, nearest-neighbors interaction, fixed boundary conditions; see Fig. 1, where dots denote moving particles, open circles represent the fixed boundary particles, and each segment corresponds to an interaction. Particles move in the plane under the influence of a molecular-type two-body potential, of the form

$$U(r) = 4U_0 \left[\left(\frac{\sigma}{r} \right)^4 - \left(\frac{\sigma}{r} \right)^2 \right], \quad (1)$$

where r is the distance between particles; in the common FPU language, this is an “ $\alpha+\beta$ ” model. Let n denote the number of degrees of freedom and $\varepsilon = E/n$ the specific energy; the main result of Ref. 1 that will have a paradigmatic role in the present paper, is reported in Fig. 2, where the equipartition time $T_n(\varepsilon)$ is plotted versus ε for different values of n . [A precise definition of $T_n(\varepsilon)$ is provided in Sec. II B; roughly, it represents the time at which a preassigned “degree of equipartition” is reached, starting from a situation in which only a small fraction of normal modes are initially excited.] As the figure suggests (see Ref. 1 and Sec. II C for a detailed analysis), for large

n the curves $T_n(\varepsilon)$ flatten on a line $T_\infty(\varepsilon)$. Moreover, the line in the log-log scale has slope 1, so for large n one gets the trivial law

$$T_\infty(\varepsilon) = C/\varepsilon. \quad (2)$$

This means that the large time scales, which are known to dominate at small ε and large n the one-dimensional problem, in this model disappear. In the present paper we continue this research in several directions: (i) We extend the study to other models, differing in particular for the boundary conditions; as we shall see, the boundary conditions turn out to be (unexpectedly) relevant. (ii) Besides FPU-like initial states, in which all energy is shared by only a few modes, we also consider states close to equipartition, and measure the time scale at which some large fluctuation of the energy of the normal modes, with respect to equipartition, is readsorbed. (iii) To show more clearly and quantitatively the differences between dimensions one and two, we add a comparison with a one-dimensional model having exactly the same potential. On the whole, these results show, in our opinion, that the FPU problem, in dimension two, is substantially different than in dimension one, and moreover, the phenomenology looks model-dependent in a more essential way.

^{a)}Electronic mail: benettin@math.unipd.it.

^{b)}Electronic mail: gradenigo@science.unitn.it.

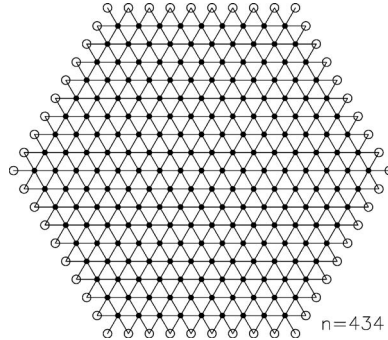


FIG. 1. The hexagonal lattice. Dots: moving particles. Open circles: a border of fixed particles. Each line connecting nearest-neighboring sites represents an interaction.

I. INTRODUCTION

A. Motivation

After the pioneering paper by Fermi, Pasta, and Ulam,² a huge amount of work has been devoted to the FPU problem, namely the problem of the energy equipartition among normal modes, or more generally the problem of the dynamical foundations of the common assumptions of classical statistical mechanics, in a weakly nonlinear lattice. The literature, in more than 50 years, is so abundant, that it is not conceivable to provide here even a poor account of it. For an updated “state of the art,” including all the relevant references, we defer to the papers collected in Refs. 3 and 4. We stress however that most of the work concerns one-dimensional models, while only a few papers concern higher dimension. (The old literature includes, to our knowledge, Refs. 5–8.

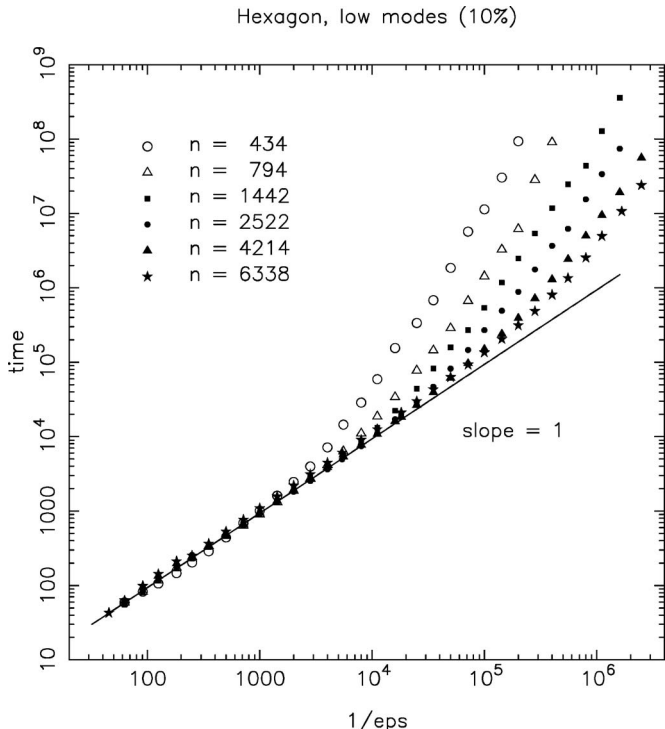


FIG. 2. The equipartition time $T_n(\epsilon)$ vs ϵ^{-1} , in the log-log scale, for the hexagonal model, for different values of n . Initial data: energy equidistributed among 10% of the modes of lowest frequency. n increases, left to right, from 434 to 6338.

Such studies, however, are performed with poor means compared to the possibilities nowadays, and do not appear to provide much help for the questions we are addressing here. More recent studies in dimension higher than one are devoted to the thermal conductivity⁹ and to the specific heat,¹⁰ questions that we do not discuss here.)

Although there is no complete agreement in the literature, the following “one-dimensional scenario” seems to be rather well established (see, in particular, Refs. 11 and 12 and, for comments, the reviews in Refs. 13 and 14):

- (i) On a first short time scale the energy, which was initially concentrated in a few modes, is spread among a larger group of them, naturally producing a “packet” of energy-sharing modes.
- (ii) The situation (the packet) is metastable and evolves very slowly towards equipartition, requiring for this quite a long time scale. (The idea that two well separated time scales enter the problem, and specifically the idea of metastability, goes back to Refs. 15 and 16. After other relevant contributions like Ref. 17, the phenomenon was reconsidered and strongly emphasized, also, in view of possibly important physical consequences, in a series of papers by the group working in Milano, among them Refs. 11 and 12. For a more complete account, see the above quoted reviews.^{13,14} In fact, the idea that different mechanisms govern the initial spreading of energy among low modes and later on, possibly, the energy distribution to all modes, goes back to the early papers on FPU; see, for example, Refs. 18 and 19, and references therein.) The particularly accurate computations in Ref. 12 concerning the β -model, indicate that the equipartition time grows as a stretched exponential of the specific energy ϵ , namely,

$$T \sim \exp 1/\epsilon^{1/4}. \quad (3)$$

As is quite important in view of a physical interpretation, the number of degrees of freedom, if sufficiently large, is irrelevant, so the scenario persists in the thermodynamic limit.

A different behavior was found in Ref. 1 for the two-dimensional hexagonal model exhibited in Fig. 1: intermediate metastable states are apparently absent, while equilibrium times, as already remarked in the leading paragraph, are substantially shorter. For large n , $T_n(\epsilon)$ converges to the trivial law $T_\infty(\epsilon)$ given by Eq. (2). After that, Carati and Galgani (private communication, 2005) made a few computations on a two-dimensional model with the same potential as in Ref. 1, but with the shape of a parallelogram and periodic rather than fixed boundary conditions; see Fig. 3, left. They observed, for certain values of n and ϵ , equipartition times longer than in Ref. 1 and suggested to us to study in a more systematic way, the FPU problem in dimension two, including their model in the study. This is indeed the origin of the present paper. Here we consider the periodic model introduced by Carati and Galgani, as well as a similar model with the same shape of a parallelogram, but with fixed boundary conditions; several computations have been also repeated on

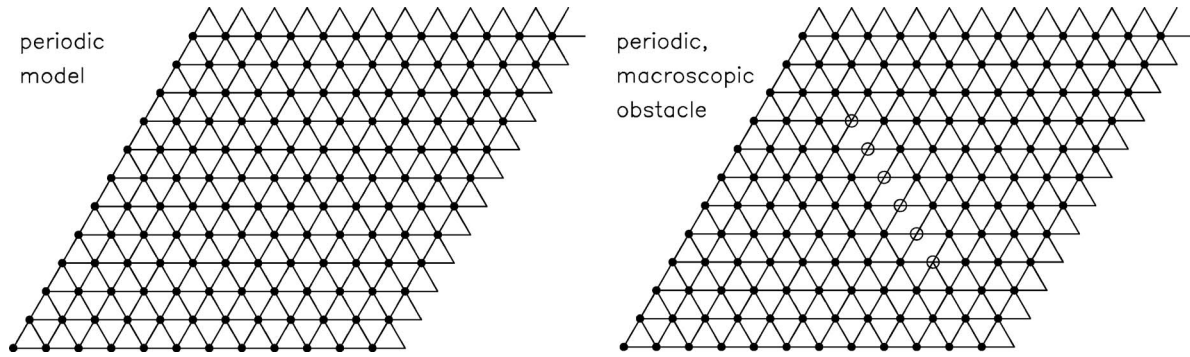


FIG. 3. Left: the parallelogram-shaped model, with periodic boundary conditions. Right: a similar periodic model, with however a line of fixed particles (open circles) occupying one half of the minor diagonal.

a model with free boundary conditions as well as on a periodic model, containing however a macroscopic obstacle, namely, a line of fixed particles occupying one half of the minor diagonal (Fig. 3, right). We restricted the attention to models with equal sides. Most computations concern “FPU-like” initial conditions very far from equilibrium, all of the energy being initially concentrated in a small fraction (10%) of the normal modes, either in the lowest or in the highest part of the spectrum. Some computations however concern states close to equilibrium, see Sec. III. For a better understanding of the difference between dimension two and one, we also studied, although not systematically, a one-dimensional model with the same potential equation (1).

B. The frequency spectrum of the considered models

All the models we studied have nearest-neighbors interaction; the Hamiltonian is

$$H(r_1, \dots, r_N, p_1, \dots, p_N) = \sum_{i=1}^N \frac{\|p_i\|^2}{2m} + V(r_1, \dots, r_N) \quad (4)$$

with

$$V(r_1, \dots, r_N) = \sum_{i,j}^{(nn)} U(\|r_j - r_i\|),$$

the two-particle potential $U(r)$ as in Eq. (1); the sum extends over all pairs of nearest-neighboring particles. The derivative U' vanishes at $r = \sqrt{2}\sigma$ and as is typical, such a distance has been taken as the lattice size (no pressure at equilibrium). We used ρ , m , and U_0 in Eq. (1) as units, respectively, of length, mass, and energy, and consequently $\rho\sqrt{m}/U_0$ as the time unit. For all models but the periodic one, the frequencies $\omega_1, \dots, \omega_n$ of the normal modes, as well as the $n \times n$ matrix W of transformation from particles to modes, have been computed numerically by diagonalizing the Hessian matrix of V . (We are not aware of any method to compute such quantities analytically.) For the periodic model instead the analytic computation is possible. For this model we made both the numerical and the analytic diagonalization (for the latter see the Appendix), checking that the results are identical up to the numerical round-off. For all models, modes are ordered by increasing frequency (only in the periodic case modes are plane waves, and could be identified by a two-

dimensional wave number and a polarization).

The frequency spectra of all two-dimensional models are found to be almost identical, see Fig. 4 (the value of n are 2522 for the hexagon and 3200 for all of the other models; n however turns out to be practically irrelevant). For comparison, the spectrum of the one-dimensional model with the same potential equation (1), is also drawn in the figure. Let us stress that the quantity reported in the figure is just ω_k versus k/n , not to be interpreted as a dispersion relation (in dimension two, k is just a counter), but as the inverse of the function $k(\omega)$ giving the number of modes up to a given frequency (the integral of the density of states); the fact that all curves in dimension two practically coincide indicates that the density of states is independent of the model. The difference with respect to dimension one is relevant in the lower part of the spectrum, which in dimension two is not

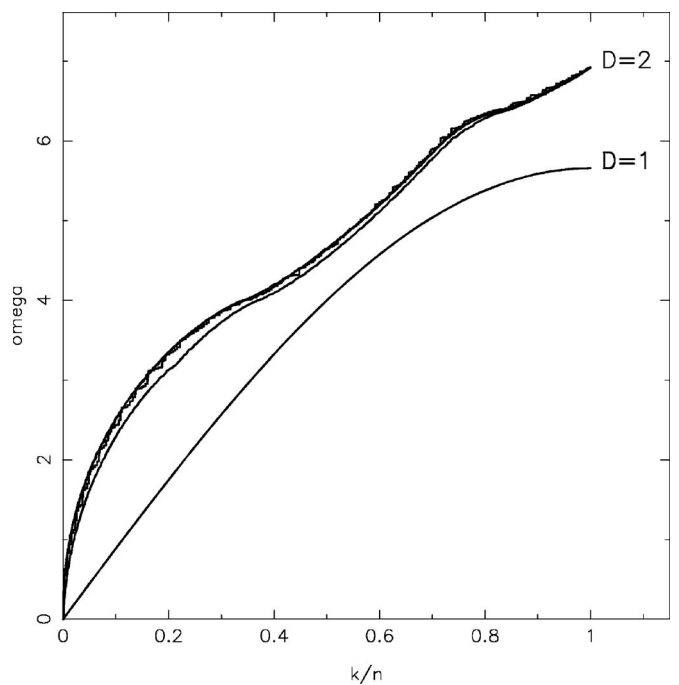


FIG. 4. The bunch of upper curves: ω_k vs k/n for the hexagonal model ($n = 2522$) and for the four parallelogram-shaped models, with periodic, fixed, free and periodic with obstacle boundary conditions ($n = 3200$). Lower curve: the same quantity for a one-dimensional model with the same potential $U(r)$.

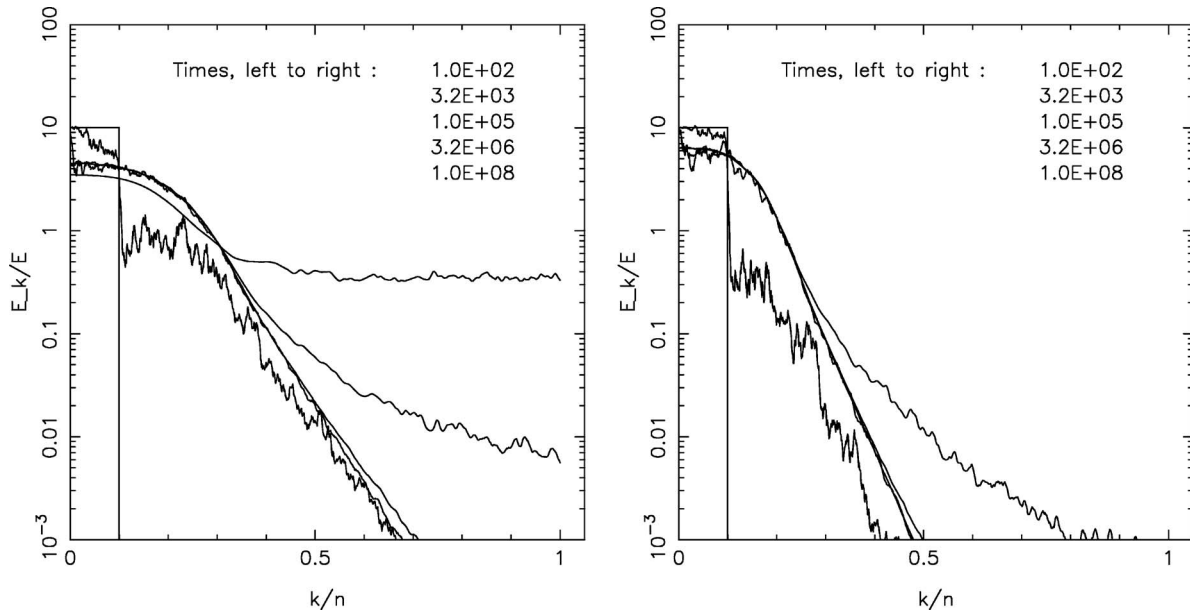


FIG. 5. The energy distribution among normal modes in dimension one, $n=1023$, at different times. Left: $\epsilon=0.5 \times 10^{-3}$; right: $\epsilon=10^{-4}$. Times, left to right: $10^2, 3.2 \times 10^3, 10^5, 3.2 \times 10^6, 10^8$.

linear (it is close to a square root), and also in the upper part of the spectrum, which is not flat. So, passing from dimension one to two the resonance properties are modified in an important way.

C. A short account of the main result

In the very essence, our main result can be summarized as follows:

- (i) In none of the two-dimensional models we have considered, there is evidence of intermediate metastable states, or more generally of the presence of more than one time scale in the problem. The process of energy sharing from the initially excited modes to all modes is gradual, and involves rather uniformly all frequencies.
- (ii) All models but the periodic parallelogram (without obstacle) behave, also quantitatively, *exactly* as the hexagonal model. For all of them the equilibrium times $T_n(\epsilon)$ (see Sec. II B for the precise definition of T_n) approach for large n a line $T_\infty(\epsilon)$ given by Eq. (1); as is remarkable, not only the ϵ -dependence, but also the constant C is practically the same for all such models.
- (iii) For the periodic parallelogram, the behavior is less clear. Equilibrium times are indeed larger than in the other two-dimensional models, but not much larger, and definitely *much* smaller than in dimension one. It should also be mentioned that, at the largest value of n we have been able to work with, namely $n=28\,800$, the large n asymptotics is not yet reached; $T_n(\epsilon)$ still decreases by increasing n . An asymptotic analysis, however, suggests a possible asymptotic law of the form $T_\infty(\epsilon) \sim \epsilon^{-5/4}$.

D. The organization of the paper

This paper is organized as follows: in Sec. II, which is the bulk of the paper, we deal with FPU-like initial conditions far from equilibrium, and explain in detail our results concerning the absence of metastability and the time scale for equipartition of the different models, with emphasis on the large n asymptotics. Section III contains instead a study of the equilibrium times for initial conditions close to equipartition, as well as some concluding remarks. The Appendix is devoted to the analytic computation of the frequency spectrum for the periodic model.

II. RESULTS FOR THE FPU-LIKE INITIAL DATA

A. The search for metastability

There are several methods, in dimension one, to make evident the formation of metastable states, i.e., states in which only some of the normal modes do appreciably share energy (see, in particular, Refs. 12 and 13). A simple way, which in our opinion provides quick qualitative evidence, consists of looking at the spectrum of the averaged energies of the modes (what follows is nothing but a poor imitation of the “movies” we could see in Milano):

$$\bar{E}_k(t) = \frac{1}{t} \int_0^t E_k(t') dt'$$

[with obvious meaning of $E_k(t)$], at different times. Figure 5 (left) shows in the semilog scale the ratio $\bar{E}_k(t)/\epsilon$ versus k/n , for the one-dimensional model with $n=1023$, at $\epsilon=5 \times 10^{-4}$, for times growing roughly in geometric progression. Initially the energy was equidistributed among the lowest 10% of the modes, with random initial phases. (The role of the initial phases for FPU-like initial conditions, in dimension one, turns out to be crucial.²⁰) One can observe that rather soon

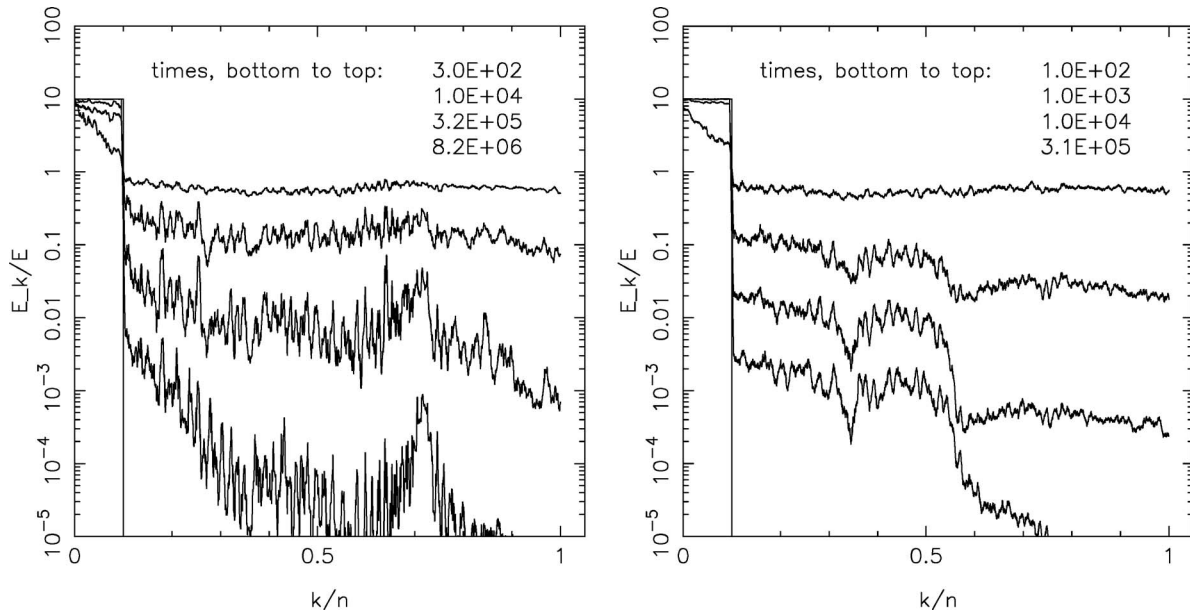


FIG. 6. The energy distribution among normal modes in dimension two, at different times. Left: periodic model, $n=12800$, $\varepsilon=2.8 \times 10^{-5}$; times, bottom to top: 3×10^2 , 10^4 , 3.2×10^6 , 8.2×10^6 . Right: hexagon, $n=6338$, $\varepsilon=10^{-5}$; times, bottom to top: 10^2 , 10^3 , 10^4 , 3×10^5 .

($t=100$, or slightly more) a well defined energy profile is formed, with a packet of energy-sharing modes followed by an exponential tail. The situation (the energy profile) remains nearly unchanged for a rather large time scale, much larger than the time needed to form the profile; after that the system slowly evolves towards equipartition, the high-frequency modes being also progressively involved in the dynamics. (The curves in the figure are a little smoothed; each point is indeed the average of a few nearby points.) The right panel of the figure shows the same phenomenon, for the same model, at lower $\varepsilon=10^{-4}$; the stability of the energy profile now extends to larger times. By further decreasing ε , one would observe an apparently perpetual freezing of the profile, after the formation of the packet. Increasing n , does not appreciably modify the figures; $n=1023$ already represents the asymptotic behavior.

Figure 6 shows the corresponding phenomenon in dimension two, for the periodic model (left) and the hexagonal model (right). Quite clearly, the behavior is qualitatively different; there is no rapid energy sharing with any packet of modes, and no exponential tail, while all modes progressively enter the game, more or less to the same extent (look in particular at the jump of the curves at $k/n=0.1$, which is not smoothed until the largest times).

A reliable indicator of the uniformity of the energy distribution among modes, is provided by the so-called “effective number of degrees of freedom” n_{eff} ,^{23,24} defined by

$$n_{\text{eff}}(t) = \exp \eta(t), \quad (5)$$

where $\eta(t)$, called spectral entropy,^{21,22,29} is in turn defined by

$$\eta(t) = - \sum_{k=1}^n P_k(t) \log P_k(t), \quad P_k(t) = \frac{\bar{E}_k(t)}{\sum_j \bar{E}_j(t)}$$

(for a comment on the use of the time averages of the energies computed from $t=0$, rather than on a shorter window, see Sec. III B, point iv). The presence of two well separated time scales in the one-dimensional dynamics is very evident, if one looks at the time behavior of n_{eff} . Figure 7, left, shows $n_{\text{eff}}(t)$ versus t for $n=1023$ and $\varepsilon=10^{-3}$, 5×10^{-4} , 10^{-4} , with energy initially equipartitioned among the lowest 10% of the modes. (The last two curves refer to the same runs as in Fig. 5.) The creation of the metastable state is evident by a quick formation of a *plateau*, which then resists for quite a long time, before the whole system moves towards equipartition. The corresponding curves for the parallelogram with periodic boundary conditions are exhibited in the right part of Fig. 7. Quite clearly, only one time scale is now visible: the two-dimensional systems do evolve in a very progressive way from the initial state to equipartition.

Very similar results are found for all the two-dimensional models we have considered. Such results indicate rather clearly, in our opinion, that the formation of a metastable intermediate state is peculiar of dimension one (although other two-dimensional models, see the concluding remarks in Sec. III B, could behave differently). Let us also observe that a theoretical description of the formation of metastable states in dimension one, based on the use of the KdV equation as a model, to a certain extent, for FPU, does exist,^{25–27} but it profits in an essential way of the peculiarities of dimension one (including the almost linearity of the lower part of the frequency spectrum). It is worthwhile to remark, however, that in a very recent paper²⁸ the notion of metastability has been reconsidered, and applied to states close to

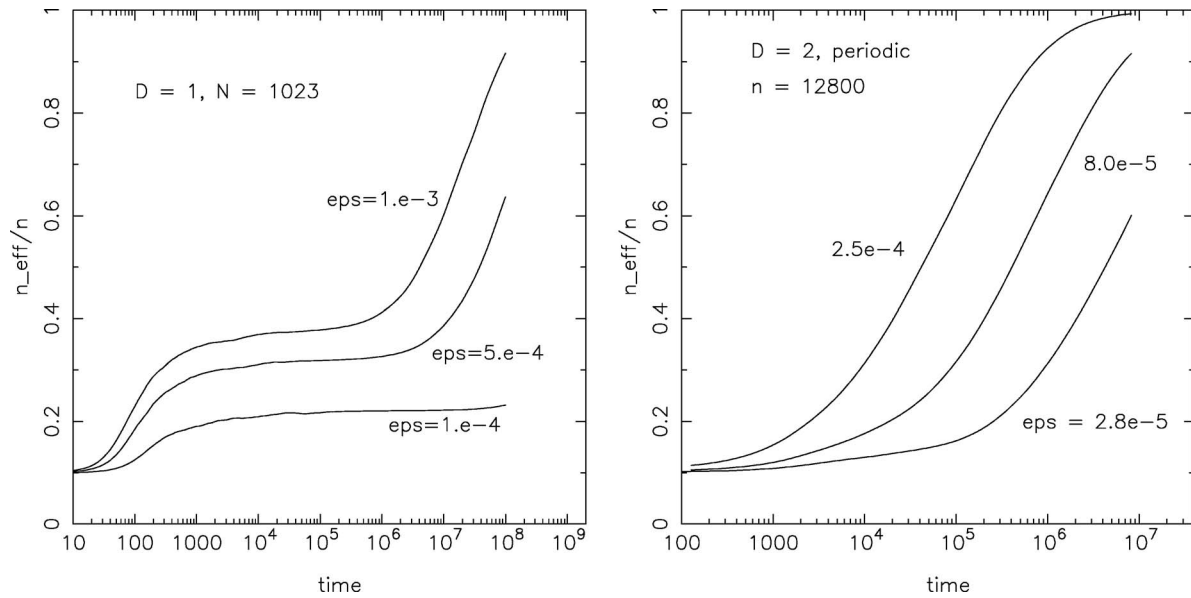


FIG. 7. The time evolution of the effective number of degrees of freedom n_{eff} , when energy is initially equipartitioned among the lowest 10% of modes, in dimension one (left) for $n=1023$ and $\varepsilon=10^{-3}$, 5×10^{-4} , 10^{-4} , and in dimension two (right) for the parallelogram with periodic boundary conditions, $n=12800$, $\varepsilon=2.5 \times 10^{-4}$, 8×10^{-5} , 2.8×10^{-5} .

equilibrium, via the observation of the time correlation of the energies of the normal modes. Whether such a reinterpretation of the notion of metastability can modify the perspective in dimension two, is in our opinion an open question which deserves further investigation.

B. The equipartition times

In this subsection, which is the core of the present paper, we study the equipartition time $T_n(\varepsilon)$ as a function of ε and n , for the different two-dimensional models we have considered. The definition we use of the equipartition time is the same we used in Ref. 1. We simply look at the time at which $n_{\text{eff}}(t)$, defined as in Eq. (5) and shown in Fig. 7, attains the (conventionally chosen) threshold 0.6, midway between the initial value and one. The already commented Fig. 2, taken from Ref. 1 shows $T_n(\varepsilon)$ versus $1/\varepsilon$, in log-log scale, at different n , for the hexagonal model. A detailed analysis of the individual curves, and specifically of the way in which curves flatten, by increasing n , on the line drawn in the figure, is reported in Ref. 1. What is relevant is that, by increasing n , a limit behavior $T_\infty(\varepsilon)$, virtually representing the equipartition times in the thermodynamic limit, apparently exists, and since the line has slope one, it is the short time equation (2). By the way, in the microscopic time units we are here using (look at the scale of frequencies in Fig. 4), the constant C is also close to one.

The four panels of Fig. 8 show the corresponding behavior of $T_n(\varepsilon)$ for the parallelograms with, in the order, periodic, fixed, free, and periodic with obstacle boundary conditions. For comparison, the line appearing in Fig. 2, representing $T_\infty(\varepsilon)$ for the hexagon, has been drawn in each panel. Quite clearly, all models but the periodic one (first panel) behave exactly as the hexagonal model, with a trivial asymptotic law of the form (2), and moreover with nearly the

same constant C . For the periodic model instead times are larger, and this deserves a further investigation.

In Fig. 9 we reported the last curves, i.e., the curves corresponding to the largest n we could work with, for the periodic model and for the parallelogram with fixed boundary conditions; for comparison, we also reported a few values of $T_n(\varepsilon)$ for the one-dimensional model with $n=511$, 1023, 2047, and 4095. (Quite clearly, in dimension one the value of n is irrelevant, in agreement with Ref. 12.) The figure shows that at the small but still reasonable value $\varepsilon \approx 0.3 \times 10^{-3}$ [recall that the depth U_0 of the potential well of the potential equation (1) is one], T_n for the two considered two-dimensional models differs only by a factor 3.5, while the corresponding T_n for the one-dimensional model is larger by a factor 2.5×10^4 . To get, in dimension two, a ratio of equipartition times as large as 40, ε must be lowered to 10^{-5} . In these conditions, for a model with 28 800 degrees of freedom, the total energy E is only 0.28, *three tenths of the potential well of a single link in the model*. It is hard to believe that such a range of energies can be of physical interest.

C. The large n asymptotics: An attempt

Apart from the above rough quantitative considerations, we made an attempt to understand the asymptotic behavior of $T_n(\varepsilon)$ for large n , looking for a curve $T_\infty(\varepsilon)$, for the different models. A similar analysis has been already performed in Ref. 1 for the hexagonal model. Here we add some scaling considerations, which will be relevant for the subsequent discussion concerning the periodic model.

In view of the asymptotic law $T_\infty(\varepsilon) \sim 1/\varepsilon$, it is interesting to look at the rescaled quantity $f(n, \varepsilon) = \varepsilon T_n(\varepsilon)$, which represents the deviation from the asymptotic law due to the finite size of the system. Figure 10, left, shows the result. Now it is rather clear that curves superimpose, if we translate

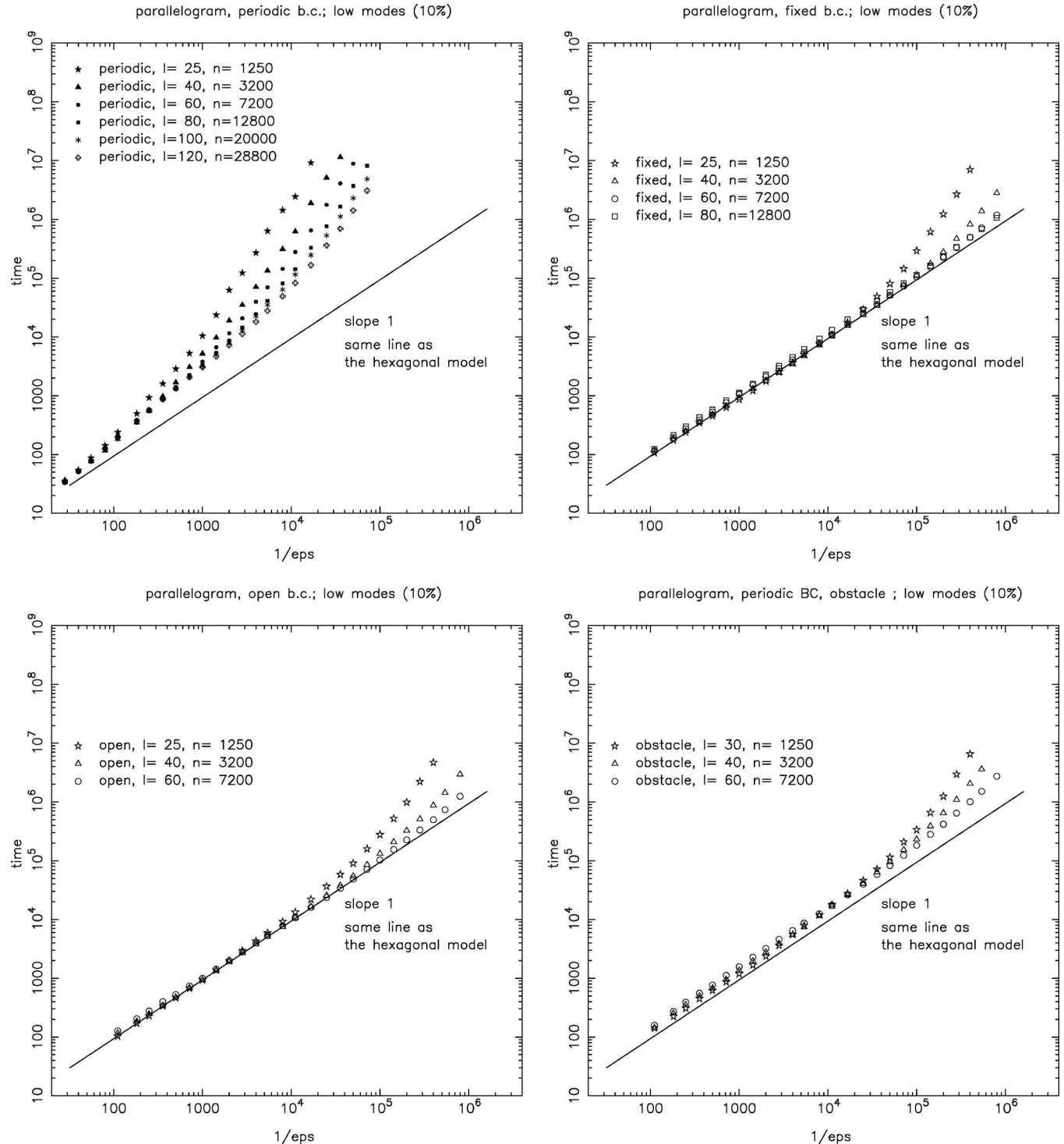


FIG. 8. $T_n(\varepsilon)$ vs $1/\varepsilon$, in the log-log scale, for the different parallelogram-shaped models, with (left to right, top to bottom) periodic, fixed, free, periodic with obstacle boundary conditions.

to the left the curves with higher n . As a matter of fact, a good superposition is obtained, see Fig. 10 right, if in place of ε we use as variable εn^γ , with $\gamma=7/4$ ($\gamma=3/2$ or 2 give definitely worse results). This suggest that $f(n, \varepsilon)$ is in fact a function of the single variable εn^γ ,

$$f(n, \varepsilon) = F(\varepsilon n^\gamma), \quad (6)$$

the n -independent function F has the profile exhibited in the right panel of Fig. 10. The overall behavior of T_n is correspondingly

$$T_n(\varepsilon) = \frac{1}{\varepsilon} F(\varepsilon n^\gamma), \quad \gamma \approx 7/4.$$

For fixed ε and large n , F converges quite fast to a constant C , and correspondingly T_n converges fast to $T_\infty = C/\varepsilon$.

Let us come to the periodic model, and look carefully at its curves $T_n(\varepsilon)$. First of all, Fig. 11 left panel, shows that for not too small ε , the curves, in the log-log scale, are well interpolated by a line. The line represented in the figure has slope $\delta=5/4$; a least-squares fit gives indeed $1.25 \leq \delta$

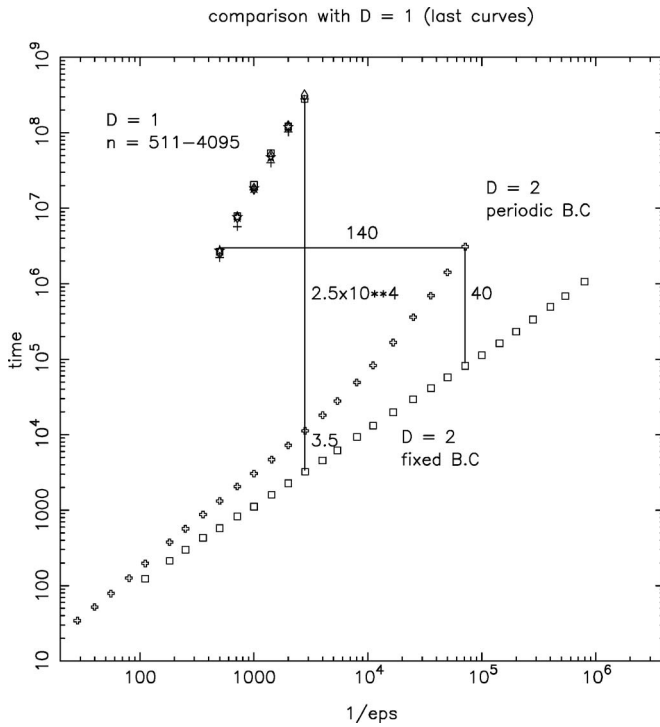


FIG. 9. $T_n(\varepsilon)$ vs $1/\varepsilon$ for the parallelograms with periodic boundary conditions ($n=28\,800$) and fixed boundary conditions ($n=12\,800$), and for the one-dimensional model ($n=511, 1023, 2047, 4095$). Some ratios of times at the same ε , and a ratio of values of ε at the same time, are indicated in the figure.

≤ 1.27 (three std. deviations), and $5/4$ has been chosen for aesthetic reasons. On the opposite side, in the region of small ε , the curves turn out to be well fitted by a stretched exponential

$$T_n(\varepsilon) \simeq c_n \exp(\varepsilon_n/\varepsilon)^{1/8}, \quad (7)$$

see Fig. 11, right. This resembles the stretched exponential law (3) occurring in dimension one¹² for the β -model, apart from the different exponent. [Such a difference should not be a surprise. The exponent $1/8$ is expected to appear in dimension one, too, for an α or $\alpha+\beta$ -model (A. Ponno, unpublished). Basically, in an α -model $\sqrt{\varepsilon}$ replaces ε everywhere.] However, at variance with dimension one, c_n and ε_n converge to nonvanishing limit values for large n , thus giving in the limit the exponential law (3). Here instead, up to the maximal $n=28\,800$ we could explore, there is no indication of a similar convergence. How do the two different behaviors match? An obvious possibility to be considered is that similar to the case of fixed boundary conditions, the different curves $T_n(\varepsilon)$ flatten, for large n , onto the above considered line with slope $\delta=5/4$. To exploit such a possibility, we tried to make for this model a convenient scaling analysis. This time we write $T_n(\varepsilon)=\varepsilon^{-\delta}f(n,\varepsilon)$, and proceed as above. We try to find a value of γ , such that Ref. 6 holds. A satisfactory result is obtained for $\gamma=5/4$, see Fig. 12 ($\gamma=1$ as well as $\gamma=3/2$ definitely give worse results). This suggests for the periodic model the behavior

$$T_n(\varepsilon) = \frac{1}{\varepsilon^{5/4}} F(\varepsilon n^{5/4})$$

and the corresponding asymptotic behavior for large n is

$$T_\infty(\varepsilon) = \frac{c}{\varepsilon^{5/4}}.$$

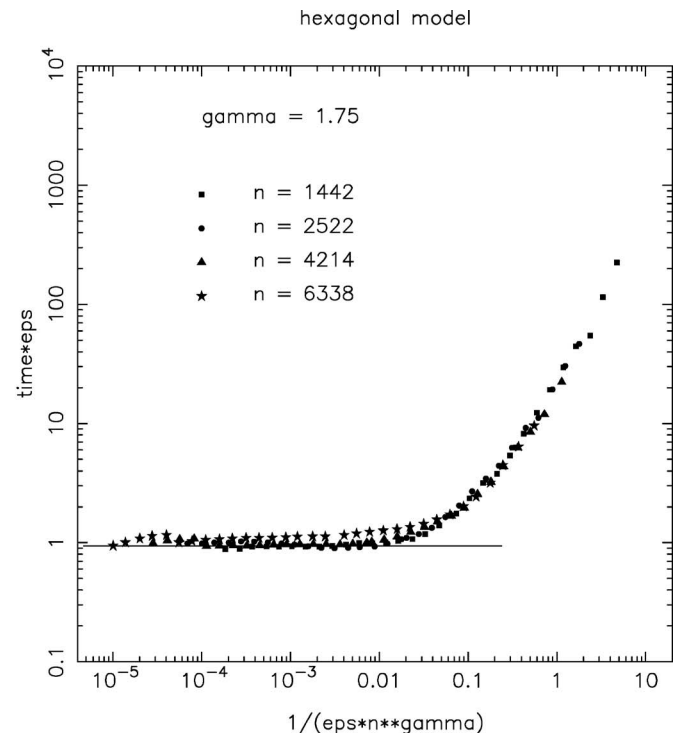
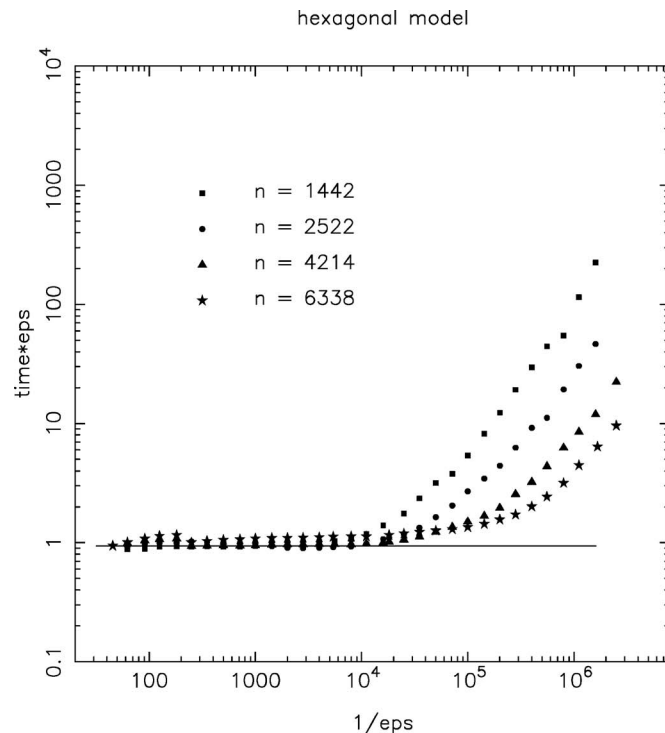


FIG. 10. $\varepsilon T_n(\varepsilon)$, for the hexagonal model, as a function of $1/\varepsilon$ (left) and of $1/(\varepsilon n^\gamma)$, $\gamma=7/4$ (right).

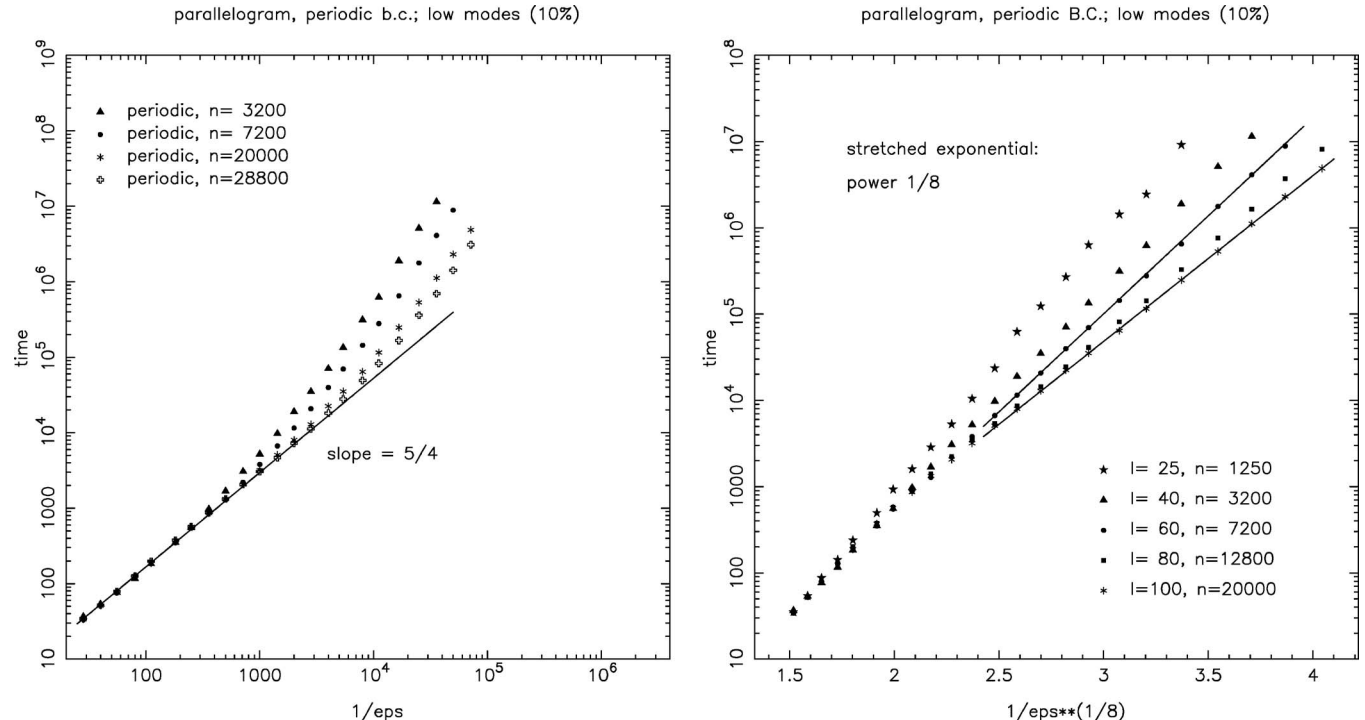


FIG. 11. Attempts to fit the large- ε behavior with a power law (left), and the small- ε behavior by a stretched exponential (right), for the periodic model.

D. Equipartition times, high-frequency modes

Although the most commonly used FPU-like initial conditions are those in which the modes of lowest frequency are excited, we decided to repeat most experiments, initially giving energy to high-frequency modes, more precisely to 10% of the modes with $0.85 \leq k/n \leq 0.95$. The results do not

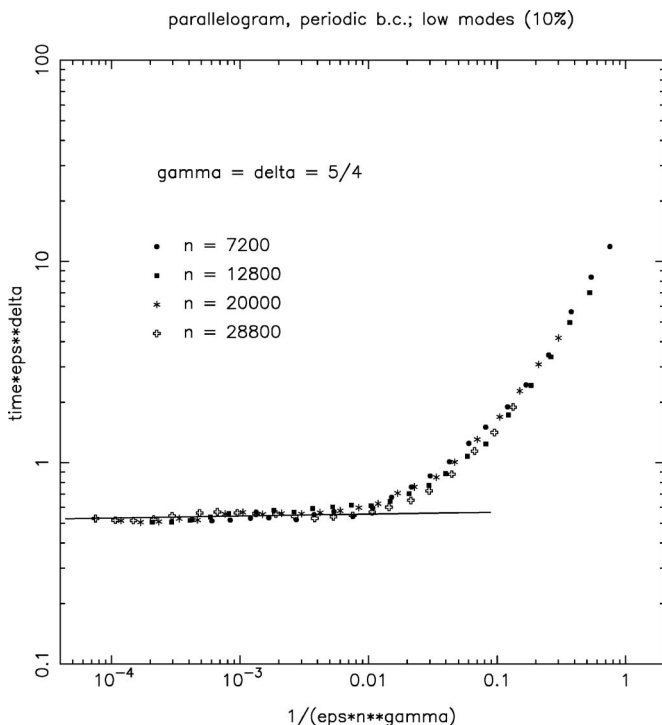


FIG. 12. The rescaled time $\varepsilon^\delta T_n(\varepsilon)$ vs $1/(\varepsilon n^\gamma)$, $\delta=\gamma=5/4$, in the log-log scale, for the periodic model.

change in a significant way. Figure 13 left, shows $T_n(\varepsilon)$ for the periodic model; the dashed line is the line with slope $5/4$ which appears, as the possible asymptotic behavior, in the left panel of Fig. 11. Quite clearly, the qualitative behavior is the same; equipartition times are just a little reduced. The right panel of Fig. 13 refers instead to the corresponding model with fixed boundary conditions. Here too, the dashed line is the asymptotic line $T_\infty(\varepsilon)$, when low modes are initially excited. The difference is clearly minor. The finite-size effect, for fixed boundary conditions, is almost negligible, apart from the smallest model with $n=1250$.

III. FURTHER RESULTS AND CONCLUDING REMARKS

A. Initial data close to equilibrium

In recent years, several papers have been devoted to the study of the FPU problem with initial conditions already close to equipartition. The basic idea is to look at fluctuations of some relevant quantities, such as the kinetic energy of the particles,²⁹ the energies of the normal modes or groups of them,^{30,10} or the energy of the whole system in a thermal bath;^{31,32} the already quoted Ref. 28 also follows this line of thought.

We did not study the question in a systematic way, but made only a few simple experiments, to get a preliminary indication of what happens in our models near equilibrium, whether the behavior exhibited in connection with the FPU-like initial conditions gets confirmed or not. We restricted the investigation to two models, namely, the parallelograms with either periodic or fixed boundary conditions. For comparison, however, we repeated the computations in the one-dimensional model. We proceeded as follows: we divided the normal modes into two groups, the low-frequency and the

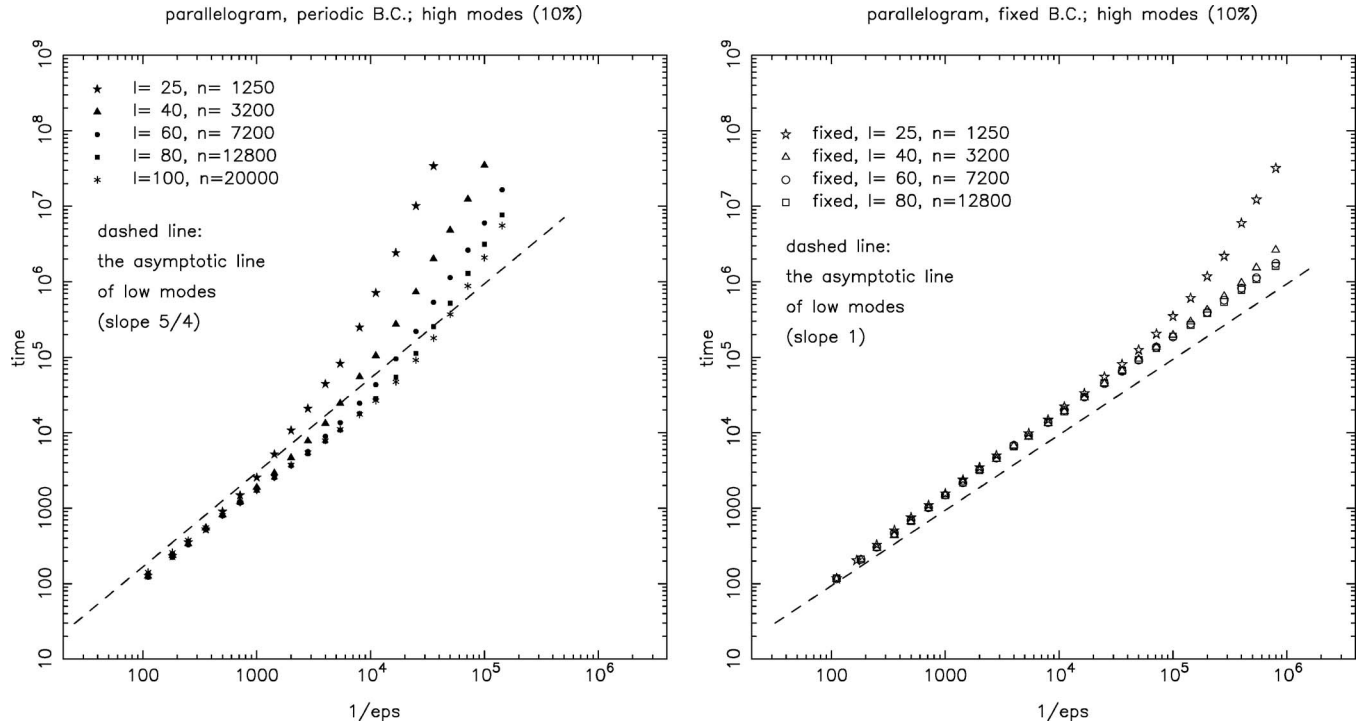


FIG. 13. The equipartition time $T_n(\epsilon)$ vs $1/\epsilon$, in the usual log-log scale, for the parallelogram with periodic (left) and fixed (right) boundary conditions. The dashed lines represent the asymptotic behavior $T_\infty(\epsilon)$, previously found for initial excitations on low modes (slopes $5/4$ and 1 , respectively, for periodic and fixed boundary conditions).

high-frequency ones, each group containing the same number of modes. We took two (inverse) temperatures β_l and β_h , respectively, for the low and the high group, with β_l larger than β_h by 20%, and randomly extracted the energy of the mode k with the Gibbs probability $\exp \beta_l E_k$ or $\exp \beta_h E_k$, depending on k . The energy per degree of freedom ϵ , in this way, is not fixed. However, thanks to the large number of degrees of freedom, the fluctuations are negligible, and ϵ in all samples of random extraction we made, was very close to the average value $\bar{\epsilon}$ corresponding to the chosen temperatures.

For each initial condition, we let the system evolve, and observed the time behavior of the energy difference ΔE , normalized to the initial value $\Delta E(0)$. As a matter of fact, the behavior of ΔE does not depend too much on the specific initial condition; to have cleaner curves, we made an average on 10 or 15 random extractions.

For dimension two, we chose β_l , β_h in such a way that $\bar{\epsilon}$ had the rather small value 10^{-5} ; for dimension one, we used instead the much larger value $\bar{\epsilon}=10^{-3}$, otherwise the decay of ΔE is too slow to be observed. Figure 14 shows the result. The curves on the right refer to the one-dimensional model. Quite clearly, ΔE decays immediately, in a time shorter than 100, from 1 to 0.95; then one observes a long *plateau*, and only on the much larger time scale $T \approx 10^7$, ΔE decays significantly towards zero. The metastability is clearly at work. The different curves correspond to three different values of n , namely $n=3\,200, 7\,200, 9\,800$; once more, in dimension one n turns out to be irrelevant (the curves, as they appear in the figure, are not even ordered with n).

The curves on the left side of the figure refer to the model with fixed boundary conditions. The values of n are

3 200, 7 200, 12 800; the times of decay are clearly much shorter, say by a factor 10^3 , in spite of the fact that $\bar{\epsilon}$ is 100 times smaller. Finally, the intermediate curves (dashed lines) refer to the two-dimensional model with periodic boundary conditions. The times are clearly larger with respect to the fixed boundary conditions, but decrease by increasing n ; the curves are indeed ordered, top to bottom, by increasing n . The values of n are 3 200, 7 200, 12 800, 20 000, 28 800.

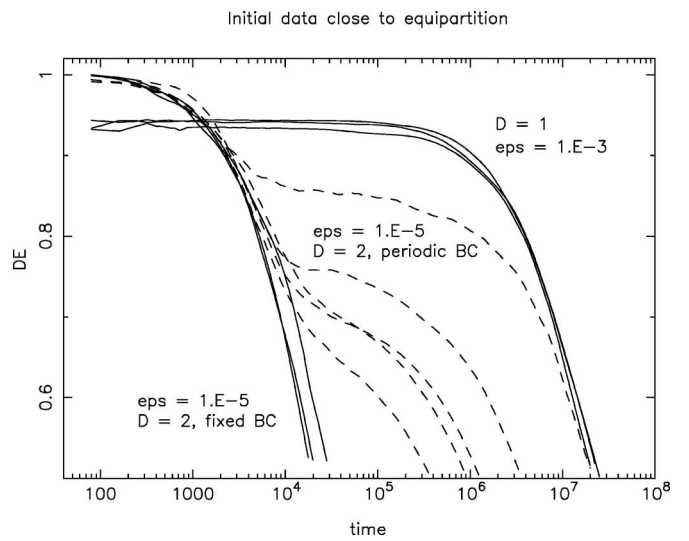


FIG. 14. The decay of the ratio $\Delta E(t)/\Delta E(0)$ vs t , for the parallelogram with fixed boundary conditions at $\bar{\epsilon}=10^{-5}$, for $n=3\,200, 7\,200, 12\,800$ (solid curves on the left); the same quantity for the periodic model at $\bar{\epsilon}=10^{-5}$, for $n=3\,200, 7\,200, 12\,800, 20\,000, 28\,800$ (dashed curves, ordered right to left) and for the one-dimensional model at $\bar{\epsilon}=10^{-3}$ (100 times larger), for $n=3\,200, 7\,200, 9\,800$ (solid curves on the right).

We plan to further study this problem (with attention at the specific heat) in the near future. Although preliminary, however, these results provide, in our opinion, a convincing indication that considering initial data close to equipartition does not change very much, at least qualitatively, the behavior of the different systems.

B. Some remarks

- (i) The first spontaneous question (actually raised by several colleagues we discussed with) is: How is it possible that the boundary conditions are so important, for large models? Indeed, Statistical Mechanics tells us that, apart from special situations like symmetry breaking in phase transitions, in the thermodynamic limit they should be irrelevant. In our opinion, this is an incomplete way to raise the question. The thermodynamic limit is indeed the limit of a macroscopic object. But the time scale one is looking at, should also be macroscopic, i.e., a double limit is necessary. If one first fixes the time, and for fixed time lets the diameter of the model to get large, then boundary conditions should be irrelevant. But in such a case, one is simply observing local phenomena that is not very interesting. If instead length and time both go to infinity in such a way that time is always (much) larger than the typical time needed for a wave to travel across the model, and wrap up around it or bounce from wall to wall, then it should be not surprising that boundary conditions are possibly important.
- (ii) For small ε , all the FPU models we have been dealing with are nearly integrable. If we pass to the normal modes coordinates P_k, Q_k , rescaled with $\sqrt{\varepsilon}$ so that the domain of the Q is ε -independent, then the Hamiltonian gets the form

$$\begin{aligned} \mathcal{H}(P, Q) = & \frac{1}{2} \sum_{k=1}^{\infty} (P_k^2 + \omega_k^2 Q_k^2) + \sqrt{\varepsilon} \mathcal{V}_3(Q) + \varepsilon \mathcal{V}_4(Q) \\ & + \dots, \end{aligned}$$

where \mathcal{V}_l is a homogeneous polynomial of degree l in Q_1, \dots, Q_n . Any difference in the dynamical behavior of the models should come from recognizable differences in \mathcal{V}_3 and possibly in the other terms. The form of \mathcal{V}_3 is well known in dimension one, while its coefficients can be studied numerically for all models in dimension two. A paper devoted to this subject is in preparation.³³ It is perhaps worthwhile to announce here that the correspondence between the structure of \mathcal{V}_3 , as described in Ref. 33 and the dynamics of the different models, is rather strict.

- (iii) All of the two-dimensional models we have considered here have a triangular cell. This is indeed the natural lattice structure, giving the closest-packing, for short-range potentials like Eq. (1). Triangular lattices are similar, in this respect, to the face-centered cubic models in dimension three. Models with the triangular cell are stable, even if one adds, for example,

second-neighbors interaction, while models with the square cell are not, if the side of the lattice is larger than a few units. A further reason to avoid squared models, is their spectrum of frequencies. Indeed in normal conditions, that is with negligible pressure, the frequencies of an $L \times L$ model with square cell are the same of a one-dimensional model of length $n=L$, each frequency having multiplicity $2L$. Such a situation looks somehow unnatural. Adding pressure so as to remove the degeneracy, seems even more unnatural. This is why, as in Ref. 1, we decided to restrict the attention to triangular lattices. There is a good chance, however, that models with square lattice, and perhaps a different potential so as to avoid instability, behave differently from models with triangular lattice,³³ and are instead more similar to one-dimensional models. This would correspond to an even stronger lack of universality in the two-dimensional FPU problem.

- (iv) A final comment concerns the procedure we used (Sec. II A) to define n_{eff} , and through it the equipartition time $T_n(\varepsilon)$. For this we made reference to the time averages $\bar{E}_k(t)$ of the energies of normal modes, computed from $t=0$; an alternative procedure would be computing the averages on a running window. A distinction here looks necessary. If the window size, although shorter, is of the same order of the overall time (for example, one third of it), in particular it grows for small ε , then no essential difference is expected. Fluctuations are averaged out, and ergodicity, if any, still results in equality of averaged energies of modes, i.e., $n_{\text{eff}}=n$; the only expected difference is that $n_{\text{eff}}(t)$ grows a little faster. If instead the size of the window is substantially smaller, say smaller than the typical correlation time of the fluctuations of the energies, then fluctuations are not averaged out, and the eventual state, even in the case of ergodicity, is not equipartition, but the presence of fluctuations, in the energy spectrum, of a standard size. This is the way chosen in Refs. 23 and 12. It is conceptually better, but it requires us to compensate for the lack of statistics due to the short averaging window, a further average on several initial data, and so it is definitely heavier from the computational point of view. Such a procedure appeared prohibitive to us, and not really necessary. Quite clearly, details could change, but the difference we observed between dimensions one and two is too substantial, to believe it is possibly due to the averaging technique.

C. Technical remarks on the numerical methods

All numerical integrations have been performed by a symplectic splitting algorithm of order four. Details can be found in Ref. 1. In the very essence, let us use, for the Hamiltonian equation (4), the compact notation $H=K+V$; the map

$$\psi_\tau = \Phi_K^{\tau/2} \circ \Phi_V^\tau \circ \Phi_K^{\tau/2},$$

where τ is the integration step and Φ_K^t, Φ_V^t denote the Hamiltonian flows of, respectively, K and V , is well known to be a symplectic algorithm of order two. If, as in our case, K depends only on the momenta and V only on the coordinates, ψ_τ is nothing but the common leapfrog. A splitting algorithm of order four is obtained by conveniently composing three algorithms of this form, namely,

$$\Psi_\tau = \psi_{c'\tau} \circ \psi_{c''\tau} \circ \psi_{c'\tau},$$

with

$$c' = \frac{1}{2 - 2^{1/3}}, \quad c'' = 1 - 2c' = -\frac{2^{1/3}}{2 - 2^{1/3}}$$

(see for the theory Refs. 34 and 35). We used this algorithm, with typically, for dimension two, $\tau=0.08$, as in Ref. 1. We checked that the results are stable by dividing τ by a factor 2 or 4. For dimension one, $\tau=0.08$ turns out to be a little too large, and to obtain stable results we had to reduce the time step to $\tau=0.04$. Such a difference is not surprising. Indeed, the one-dimensional model, as we have seen, is “more integrable” than the two-dimensional ones, and for this reason, in our opinion, it needs to be treated numerically in a more delicate way.

Concerning the numerical diagonalization of the Hessian matrix of the potential V , we used as in Ref. 1 the routines of the *Math Kernel Library* associated with the *Intel Fortran Compiler*. Due to the nearest-neighbor interaction, the Hessian matrix A is sparse. We diagonalized matrices up to $28\,800 \times 28\,800$, checking after diagonalization that $Au - \lambda u = 0$ within the round-off (in place of zero, we find a number of the order 10^{-14}). For the periodic model, for which the analytic diagonalization is possible, we verified that the analytical and the numerical diagonalization give (within the round-off) the same spectrum and the same eigenvectors, up to degeneracy.

ACKNOWLEDGMENTS

We are deeply indebted to A. Carati and L. Galgani for suggesting to us the possible relevance of the boundary conditions in the equilibrium times, as well as for their helpful criticism. We also wish to thank D. Bambusi, G. Gallavotti, A. Giorgilli, R. Livi, A. Maritan, and A. Ponno for many stimulating discussions, during the long elaboration of these results. A special thanks is due to A. Ponno for a critical review of the manuscript. This work has been partially supported by MiUR (PRIN Program No. 2005017208, 2005).

APPENDIX: ANALYTIC DIAGONALIZATION OF THE PERIODIC MODEL

Let us consider a periodic lattice \mathcal{L} as in Fig. 3 left, of possibly different sides L_1 and L_2 , generated by the pair of vectors

$$a_1 = \rho(1, 0), \quad a_2 = \rho\left(\frac{1}{2}, \frac{\sqrt{3}}{2}\right),$$

i.e.,

$$\mathcal{L} = \{x = l_1 a_1 + l_2 a_2, 0 \leq l_1 < L_1, 0 \leq l_2 < L_2\}.$$

Denoted by $q_x \in \mathbb{R}^2$ the displacement from x of the particle having x as the equilibrium position. The linearized equations of motion we are confronted with, can be written in the form

$$\ddot{q}_x = \Omega^2 \sum_{j=1}^6 \left[\frac{a_j}{\rho} \cdot (q_{x+a_j} - q_x) \right] \frac{a_j}{\rho},$$

where

$$\Omega^2 = \frac{U''(\rho)}{m} = \frac{8U_0}{mp^2}$$

and a_1, \dots, a_6 are the vectors connecting the lattice site x to the neighboring ones, namely, a_1, a_2 are as above, $a_3 = a_2 - a_1$ and $a_{i+3} = -a_j$, $j=1, 2, 3$; the dot denotes the usual scalar product.

The reciprocal lattice \mathcal{K} is generated by the reciprocal base b_1, b_2 such that $b_i \cdot a_j = 2\pi/L_j \delta_{ij}$, namely,

$$b_1 = \frac{2\pi}{L_1 \rho} \left(1, -\frac{1}{\sqrt{3}}\right), \quad b_2 = \frac{2\pi}{L_2 \rho} \left(0, \frac{2}{\sqrt{3}}\right);$$

precisely it is

$$\mathcal{K} = \{\kappa = k_1 b_1 + k_2 b_2, 0 \leq k_1 < L_1, 0 \leq k_2 < L_2\}.$$

The rather standard procedure of diagonalization (see, for example, Ref. 36) is based on the search of solutions in the form of plane waves, for example, using the complex form,

$$q_x(t) = ue^{i(\kappa \cdot x - \omega t)}, \quad \kappa \in \mathcal{K},$$

with suitable amplitude u and frequency ω . By inserting this expression in the equations of motion the rhs assumes the form

$$\frac{\Omega^2}{\rho^2} \sum_{j=1}^3 e^{i(\kappa \cdot x - \omega t)} [e^{i\kappa \cdot a_j} + e^{-i\kappa \cdot a_j} - 2](u \cdot a_j) a_j;$$

after trivial work one is then led, for each $\kappa \in \mathcal{K}$, to the two-dimensional eigenvalue equation

$$A(\kappa)u = \omega^2 u,$$

where $A(\kappa)$ is the linear operator acting on u as

$$A(\kappa)u = \frac{4\Omega^2}{\rho^2} \sum_{j=1}^3 S_j(\kappa)(u \cdot a_j) a_j,$$

having denoted

$$S_j(\kappa) = \sin^2 \frac{\kappa \cdot a_j}{2}, \quad j = 1, 2, 3.$$

In coordinates, A is the matrix

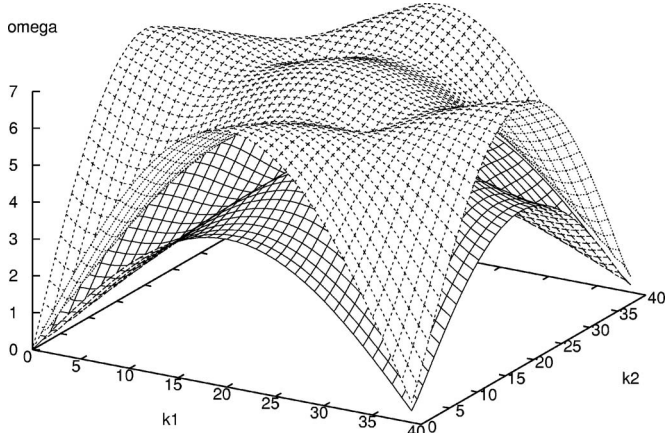


FIG. 15. The dispersion relation, namely $\omega_{\pm}(\kappa)$ vs the integer coordinates of κ in the reciprocal lattice, for the two-dimensional periodic model with $L_1=L_2=40$.

$$A = \begin{pmatrix} S_1 + \frac{1}{4}S_2 + \frac{1}{4}S_3 & \frac{\sqrt{3}}{4}(S_2 - S_3) \\ \frac{\sqrt{3}}{4}(S_2 - S_3) & \frac{3}{4}(S_2 + S_3) \end{pmatrix}.$$

For each $\kappa \in \mathcal{K}$ one finds two eigenvalues

$$\omega_{\pm}^2(\kappa) = 2\Omega^2(S_1 + S_2 + S_3 \pm \sqrt{S_1^2 + S_2^2 + S_3^2 - S_1S_2 - S_1S_3 - S_2S_3}),$$

$$S_j = S_j(\kappa).$$

This is the dispersion relation of the model. The corresponding eigenvectors $u_{\pm}(\kappa)$ provide, for each k , the two polarizations of the wave. The maximum in the above expression is attained when two of the S_j 's are 1 and the third vanishes; for ρ , m , and U_0 taken as units, it is $\omega_{\max} = \sqrt{48} \approx 6.9$.

Figure 15 provides a three-dimensional graph of the dispersion relation, for $L_1=L_2=40$. Three maxima (pay attention to the periodicity) are clearly present, in the upper branch. Both branches are acoustic, namely touch the zero. If instead the frequencies are ordered by increasing values, they assume the profile exhibited in Fig. 4.

It is an easy matter to pass from plane waves to normal modes, and work out in particular the matrix of the passage from the particles to the modes coordinates. We skip the details.

¹G. Benettin, "Time-scale for energy equipartition in a two-dimensional FPU model," Chaos **15**, 015108 (2005).

²E. Fermi, J. Pasta, and S. Ulam, "Studies of non linear problems," Los Alamos Report No. LA-1940 (1955); later published in *E. Fermi, Collected Papers* (Chicago, 1965); and Lect. Appl. Math. **15**, 143–156 (1974).

³Chaos focus issue: "The 'Fermi–Pasta–Ulam' problem—The first 50 years," Chaos **15**(1) (2005).

⁴*The Fermi–Pasta–Ulam Problem. A Status Report*, Lecture Notes in Physics No. 728, edited by G. Gallavotti (Springer, Berlin, 2008).

⁵H. Hirooka and N. Saito, "Computer studies in on the approach to thermal equilibrium in coupled anharmonic oscillators. I. Two dimensional case," J. Phys. Soc. Jpn. **26**, 624–630 (1968).

⁶P. Bocchieri and F. Valz-Gris, "Ergodic properties of an anharmonic two-dimensional crystal," Phys. Rev. A **9**, 1252–1256 (1974).

⁷G. Benettin, G. Lo Vecchio, and A. Tenenbaum, "Stochastic transition in two-dimensional Lennard-Jones systems," Phys. Rev. A **22**, 1709–1722 (1980).

⁸G. Benettin and A. Tenenbaum, "Ordered and stochastic behavior in a two-dimensional Lennard-Jones system," Phys. Rev. A **28**, 3020–3029 (1983).

⁹A. Lippi and R. Livi, "Heat conduction in two-dimensional nonlinear lattices," J. Stat. Phys. **100**, 1147–1172 (2000).

¹⁰G. Marcelli and A. Tenenbaum, "Quantumlike short-time behavior of a classical crystal," Phys. Rev. E **68**, 041112 (2003).

¹¹L. Berchiella, L. Galgani, and A. Giorgilli, "Localization of energy in FPU chains," Discrete Contin. Dyn. Syst. **11**, 855–866 (2004).

¹²L. Berchiella, A. Giorgilli, and S. Paleari, "Exponentially long times to equipartition in the thermodynamic limit," Phys. Lett. A **321**, 167–172 (2004).

¹³A. Carati, L. Galgani, and A. Giorgilli, "The Fermi–Pasta–Ulam problem as a challenge for the foundations of physics," Chaos **15**, 015105 (2005).

¹⁴G. Benettin, A. Carati, L. Galgani, and A. Giorgilli, "The Fermi–Pasta–Ulam problem and the metastability perspective," in *FPU Fifty Years Later*, edited by G. Gallavotti (Springer, Berlin, 2007).

¹⁵E. Fucito, F. Marchesoni, E. Marinari, G. Parisi, L. Peliti, S. Ruffo, and A. Vulpiani, "Approach to equilibrium in a chain of nonlinear oscillators," J. Phys. (France) **43**, 707–713 (1982).

¹⁶R. Livi, M. Pettini, S. Ruffo, M. Sparpaglione, and A. Vulpiani, "Relaxation to different stationary states in the Fermi–Pasta–Ulam model," Phys. Rev. A **28**, 3544–3552 (1983).

¹⁷M. Pettini and M. Landolfi, "Relaxation properties and ergodicity breaking in nonlinear Hamiltonian dynamics," Phys. Rev. A **41**, 768–783 (1990).

¹⁸T. P. Weissert, *The Genesis of Simulation in Dynamics: Pursuing the Fermi–Pasta–Ulam Problem* (Springer, New York, 1977).

¹⁹G. P. Berman and F. M. Izrailev, "The Fermi–Pasta–Ulam problem: Fifty years of progress," Chaos **15**, 015104 (2005).

²⁰G. Benettin, R. Livi, and A. Ponno, "The crucial role of initial phases in the one-dimensional FPU problem" (preprint, 2007).

²¹R. Livi, M. Pettini, S. Ruffo, M. Sparpaglione, and A. Vulpiani, "Equipartition threshold in nonlinear large Hamiltonian systems: The Fermi–Pasta–Ulam model," Phys. Rev. A **31**, 1039–1045 (1985).

²²R. Livi, M. Pettini, S. Ruffo, and A. Vulpiani, "Further results on the equipartition threshold in nonlinear large Hamiltonian systems," Phys. Rev. A **31**, 2740–2742 (1985).

²³J. De Luca, A. J. Lichtenberg, and S. Ruffo, "Energy transition and time scales to equipartition in the Fermi–Pasta–Ulam oscillator chain," Phys. Rev. E **51**, 2877–2885 (1995).

²⁴C. G. Goedde, A. J. Lichtenberg, and M. A. Lieberman, "Chaos and the approach to equilibrium in a discrete sine-Gordon equation," Physica D **59**, 200–225 (1992).

²⁵A. Ponno, "Soliton theory and the Fermi–Pasta–Ulam problem in the thermodynamic limit," Europhys. Lett. **64**, 606–612 (2003).

²⁶A. Ponno and D. Bambusi, "Korteweg–de Vries equation and energy shearing in Fermi–Pasta–Ulam," Chaos **15**, 015107 (2005).

²⁷D. Bambusi and A. Ponno, "On metastability in FPU," Commun. Math. Phys. **264**, 539–561 (2006).

²⁸A. Carati, L. Galgani, A. Giorgilli, and S. Paleari, "FPU phenomenon for generic initial data" (preprint, 2007).

²⁹R. Livi, M. Pettini, S. Ruffo, and A. Vulpiani, "Chaotic behavior in nonlinear Hamiltonian systems and equilibrium statistical mechanics," J. Stat. Phys. **48**, 539–559 (1987).

³⁰A. Perrone and A. Tenenbaum, "Classical specific heat of an atomic lattice at low temperature, revisited," Phys. Rev. E **57**, 100–107 (1998).

³¹A. Carati and L. Galgani, "On the specific heat of the Fermi–Pasta–Ulam systems and their glassy behavior," J. Stat. Phys. **94**, 859–869 (1999).

³²A. Carati, P. Cipriani, and L. Galgani, "On the definition of temperature in FPU systems," J. Stat. Phys. **115**, 1119–1130 (2004).

³³G. Benettin and A. Ponno (in preparation).

³⁴H. Yoshida, "Construction of higher order symplectic integrators," Phys. Lett. A **150**, 262–268 (1990).

³⁵E. Hairer, C. Lubich, and G. Wanner, *Geometric Numerical Integration* (Springer-Verlag, Berlin, 2002).

³⁶R. A. Smith, *Wave Mechanics of Crystalline Solids* (Chapman and Hall, London, 1961).